



Geochemical monitoring in the Marmara region (NW Turkey): A search for precursors of seismic activity

Sedat İnan,¹ Tayfun Akgül,^{1,2} Cemil Seyis,¹ Ruhi Saatçılar,¹ Süleyman Baykut,²
Semih Ergintav,¹ and Mahmut Baş³

Received 6 June 2007; revised 4 October 2007; accepted 5 December 2007; published 1 March 2008.

[1] Physical and chemical properties of warm and hot spring waters as well as soil radon concentrations were measured continuously during a 3-year period in the Marmara region; following the devastating İzmit earthquake of 17 August 1999 ($M_w = 7.4$). Promising and encouraging anomalies in ground radon emanation have been recorded and found to be closely related to seismic activity. The temporal and spatial variations in the soil radon data are presented. The earthquakes with magnitude >4 in the region were correlated with positive radon anomalies. Furthermore, during quiescence (absence of seismic activity) the radon data indicate random walk behavior of radon in soil and show Rayleigh-type probability density function (pdf), however, during the earthquake build-up period, the data show deviations from Rayleigh-type pdf. The radon positive anomalies indicate disturbance of the path of gas movement or gas release pattern prior to earthquakes. However, systematic and consistent anomalies in physical and/or chemical properties of the spring waters have not been detected for earthquakes occurring in the observation period ($M < 5.3$).

Citation: İnan, S., T. Akgül, C. Seyis, R. Saatçılar, S. Baykut, S. Ergintav, and M. Baş (2008), Geochemical monitoring in the Marmara region (NW Turkey): A search for precursors of seismic activity, *J. Geophys. Res.*, *113*, B03401, doi:10.1029/2007JB005206.

1. Introduction

[2] Following the devastating İzmit earthquake of 17 August 1999 with magnitude of $M_w = 7.4$ causing as many as 20,000 fatalities, geochemical observations were started in the Marmara region; in addition to existing seismological and GPS networks. Systematic monitoring of physical and chemical properties of spring waters and soil radon activity has been realized, by cooperation of TUBITAK Marmara Research Center and Istanbul Metropolitan Municipality, continuously between 2002 and 2005 at strategically located stations in the Marmara region (NW Turkey) covering an area of 40,000 km²; 400 km E-W and about 100 km N-S direction (Figure 1). Information on locations of the monitoring sites is given in Table 1. Both cold and hot springs emanating from fractures and fault zones have been sampled on daily basis and variations in anion/cations and O and D isotopes have been monitored. The variations in temperature, electrical conductivity have been continuously monitored on hourly basis. We also tried to continuously monitor spring water-radon but our attempt was unsuccessful because of inappropriate instruments for continuous

operations. Thus we concentrated our efforts on soil radon gas monitoring. Soil radon gas activity was monitored with data collected at 15 m integration time. All radon-monitoring stations and the majority of the spring water-monitoring stations were operated “online”. The data from all online stations were transferred to the center, evaluated and interpreted in the light of seismic activity on a daily basis. So far, no reliable anomaly has been detected in spring waters’ parameters that may be utilized as pre-earthquake indicator, probably due to the fact that the largest earthquake in the region did not exceed $M 5.0$ since the systematic observations were started in 2002. Also major crustal deformations detectable by geodesic techniques leading to extensive water-rock interaction have not occurred. By contrast, temporal variations of radon data suggest quite good correlation with seismic activity. Hence soil radon measurements have been continued as a promising precursor of seismic activity in the Marmara Region.

[3] Geochemical observations in search of earthquake precursors were initiated in late 1960s [Wakita, 1996]. Ever since, many reports of precursory anomalies have been published [King, 1986; Toutain and Baubron, 1999; Claesson *et al.*, 2004; Hartmann and Levy, 2005, and references therein]. On the basis of a review of earthquake precursors, Turcotte [1991] has concluded that there are no reliable precursors preceding large earthquakes. Moreover, Geller *et al.* [1997] have claimed that earthquakes cannot be predicted. However, measurements of the temporal variation of soil radon have been reported to be related to seismic and volcanic activity [Sultankhodhaev, 1984; Virk and Singh,

¹TUBITAK Marmara Research Center, Earth and Marine Sciences Institute, Gebze-Kocaeli, Turkey.

²Istanbul Technical University, Department of Electronics and Communications Engineering, Maslak, İstanbul, Turkey.

³Istanbul Metropolitan Municipality, Department of Earthquake and Ground Investigations, Saraçhane, İstanbul, Turkey.



Figure 1. Map of the study area and distribution of continuous soil gas radon monitoring and spring water monitoring stations. Black lines are the branches of the North Anatolian Fault System in the Marmara region (Faults on land modified from Şaroğlu *et al.* [1992]; faults in the Marmara Sea modified from Rangin *et al.* [2001]). Also shown are the epicenters of earthquakes $M \geq 4.0$ occurring between 2002 and 2005 in the Marmara region. (For more info see Table 2).

1993; Wakita *et al.*, 1988; King *et al.*, 1995; Toutain and Baubron, 1999; Thomas *et al.*, 1992; Chyi *et al.*, 2001; Martin-Luis *et al.*, 2002; Planinic *et al.*, 2004, among many others]. Proposed mechanisms for an increase in radon release prior to seismic and/or volcanic activity are princi-

pally: 1) rise of magma [Flerov *et al.*, 1986], 2) rise of the hydrothermal system in the crust carrying radon to shallower levels [Hauksson, 1981; Hauksson and Goddard, 1981], 3) variations in permeability of the rocks underlying soil horizon, e.g., opening and closing of microcracks due to changes

Table 1. Continuous Soil Radon and Spring Water Monitoring Stations in the Marmara Region

Soil Radon Monitoring Stations						
No	Station name	Basement Lithology	Soil Thickness (m)	Coordinates		Date of establishment dd/mm/yyyy
				Longitude	Latitude	
1	Gölcük, Şarköy, Tekirdağ	Sedimentary	~2.0	27.091	40.682	14.02.2005
2	Gaziköy, Tekirdağ	Sedimentary	~1.5	27.325	40.748	12.01.2003
3	Gönen, Balıkesir	Volcanics	~3.0	27.593	40.210	29.09.2004
4	Yenice, Çanakkale	Sedimentary	~3.0	27.294	39.930	01.12.2004
5	Susurluk, Balıkesir	Sedimentary	~3.0	28.133	40.093	09.07.2003
7	Balıkesir Ilica	Metamorphics	~1.5	27.771	39.876	14.02.2002
8	Uluabat, Bursa	Sedimentary	~2.0	28.793	40.173	22.06.2005
9	Armutlu; Yalova	Volcanics	~1.0	28.838	40.544	10.12.2001
10	Gökçedere, Yalova	Volcanics	~1.0	29.171	40.607	22.06.2005
11	Dağyenice, Çatalca	Sedimentary	~2.0	28.488	41.272	04.12.2004
12	Gebze, Kocaeli	Sedimentary	~1.0	29.450	40.786	04.07.2005
13	Donanma, Gölcük, İzmit	Sedimentary	~1.5	29.799	40.726	06.12.2004
14	Mekece, İzmit	Sedimentary	~2.0	30.049	40.454	05.12.2004
15	Adapazarı	Sedimentary	~3.0	30.379	40.709	05.12.2004
16	Efteni, Düzce	Volcanics	~1.5	31.027	40.760	20.11.2002
17	Hersek; yalova	Sedimentary	~1.0	29.513	40.722	25.08.2005
18	Dokurcun, Akyazı	Volcanics	~1.0	30.865	40.573	20.09.2005
19	Kestel, Bursa	Metamorphics	~2.5	29.218	40.181	06.10.2005
20	Saroz, Kavak, Şarköy	Sedimentary	~2.0	26.915	40.624	18.11.2002

Spring Water Monitoring Stations					
No	Station Name	Temperature °C	Coordinates		Date of establishment dd/mm/yyyy
			Longitude	Latitude	
1	Akalan, Çatalca	14.1	28.418	41.260	23.08.2002
2	Hamidiye, İstanbul	14.2	28.917	41.146	08.10.2001
3	Tuzla, İstanbul	19.6	29.296	40.844	02.10.2001
4	Efteni, Gölyaka, Düzce	41.6	31.027	40.760	13.06.2002
5	Soğucak, Yalova	21.2	29.278	40.593	26.10.2001
6	Gemlik, Bursa	36.4	29.163	40.422	04.10.2001
7	Termal, Yalova	63.5	29.170	40.603	15.06.2005
8	Ilica, Balıkesir	60.4	27.771	39.876	14.10.2001

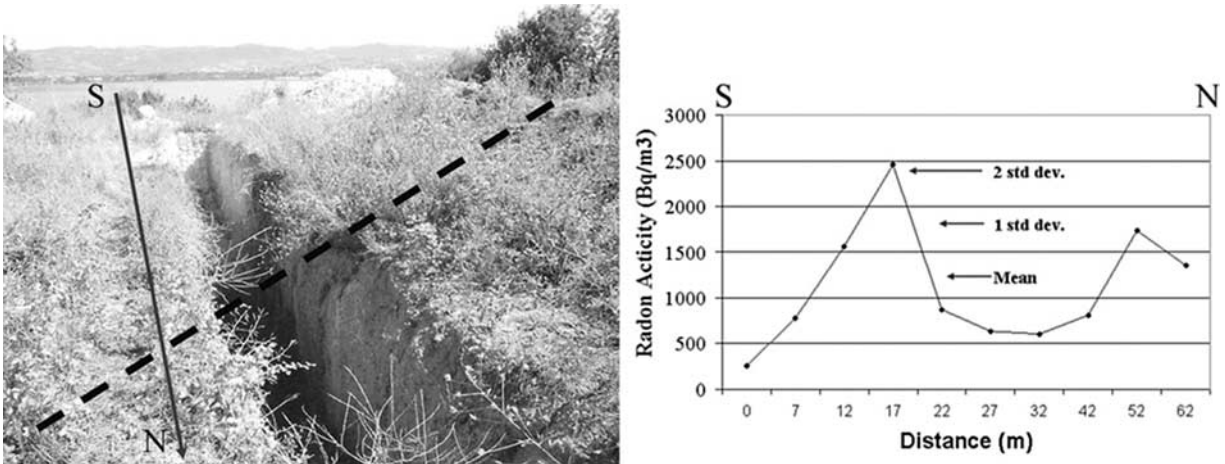


Figure 2. Spot soil gas radon measurements conducted along a profile perpendicular to a suspected fault trace for determination of best site for continuous radon monitoring station. Heavy dashed line depicts the suspected fault.

in the pre-seismic and co-seismic stress field [Heiligmann *et al.*, 1997] and 4) sweeping of radon by p-hole charge carriers generated due to rock deformation prior to impending earthquake [Freund, 2002]. All mechanisms mentioned so far have scientific merit, yet still require verification. Independent of the mechanisms leading to an increase in radon release, this study first discusses the temporal and spatial variations of soil radon in relation to seismic activity, then presents a statistical treatment of the data. Finally, a possible mechanism governing the movement of radon during quiescence and pre-seismic activity is discussed.

2. Spring Water and Soil Radon Measurements

2.1. Selection and Installations of Continuous Spring Water and Soil Radon Monitoring Sites

[4] Except in its northern parts, the Marmara region contains several warm and hot springs naturally flowing to the surface. Most of these springs are utilized in resort establishments. Many of the springs were monitored for at the least for six months before the final decision on continuous monitoring was made. During these six months several measurements of water temperature and electrical conductivity were collected continuously. Springs that did not show any major daily and/or seasonal variations were selected as initial candidates for continuous monitoring and once a good local support was provided, the site locations were finalized and continuous monitoring was started. After selection of the best sites (with the least variations in the water composition), the sensors were placed in a closed and protected water pool and the data cable connected to onsite data logger and the data transfer unit.

[5] As shown in Figure 1, the North Anatolian Fault branches in the Marmara region [Barka and Kadinsky-Cade, 1988; Şaroğlu *et al.*, 1992; Rangin *et al.*, 2001]. To get the best spatial distribution of soil radon stations, most of the fault traces were visited and spot radon measurements were made along a profile normal to the fault trace as shown in Figure 2. The maximum radon emanation point along the profile was interpreted to be best representing the fault/fracture emanation and thus was selected for the continuous

monitoring. The best site selection that is a pre-requisite for quality and sensible data collection [Chyi *et al.*, 2001] was made accordingly. After selection of the sites, shallow boreholes (0.8 to 1 meter) in soils were dug, the radon sensors were placed and covered by soil and the data cable connected to onsite data logger and the data transfer unit (Figure 3).

2.2. Instrumentation and Laboratory Analyses

[6] Daily bottled spring water from the springs were collected monthly during site visits and 30 daily samples from each spring were brought to the laboratory where they were analyzed for anions and cations using Ion Chromatography instruments (Dionex DX600). Weekly samples from all spring monitoring sites were also analyzed for O and D isotopes by EA-IRMS system (Micromass UK). IAE standards were used to calibrate the instrument.

[7] Soil radon ^{222}Rn was measured continuously at 15 min interval using alpha particle detectors (model 611 AlphaMeter, manufactured by AlphaNuclear Corporation, Canada). In this study, use of Polyethylene diffusion barrier at the bottom of the sensor ensured the exclusion of the short-lived ^{220}Rn isotope. Moreover, due to the low ionization efficiencies of beta and gamma emissions from other radionuclides compared to the alpha particles generated by the ^{222}Rn decay, the pulses generated in the detector by beta and gamma emissions are much weaker [Thomas *et al.*, 1992]. The details of the AlphaMeter and advantage of using this sensor has been discussed by Thomas *et al.* [1992]. BARASOL sensors (Model BMC2 manufactured by ALGADE Corporation France) were also used. An advantage of the BMC2 probes was claimed to be the ability to measure the soil temperature, barometric pressure and surface precipitation.

2.3. Quality Control of the Data

[8] Laboratory analyses of the spring waters for anions/cations were made using Ion Chromatography, and analyses for stable isotopes of O and H were made by EA_IRMS in conjunction with instrument performance checks using international standards with certificates. The temperature,



Figure 3. Soil Radon Site selection and deployment of continuously recording radon sensor and establishment of data recording and transfer unit.

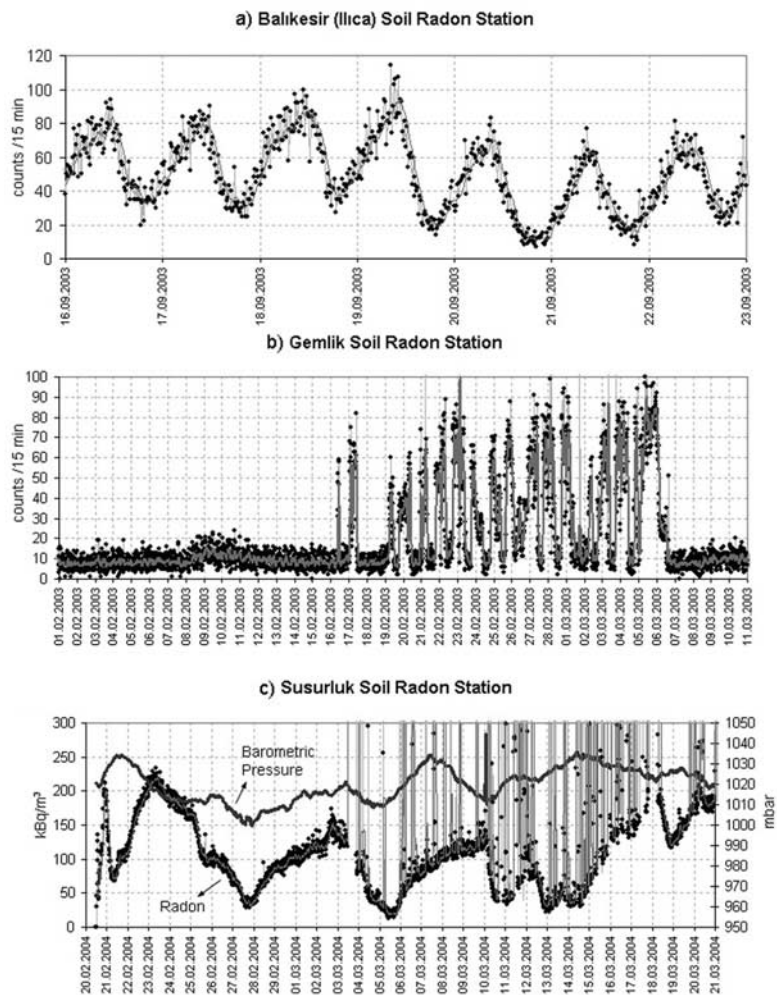


Figure 4. Adverse effect of unstable power supply (a) quarry blast (b), and humidity (c) on the performance of radon sensor. Blue line in Figure 4c is the barometric pressure in the borehole.

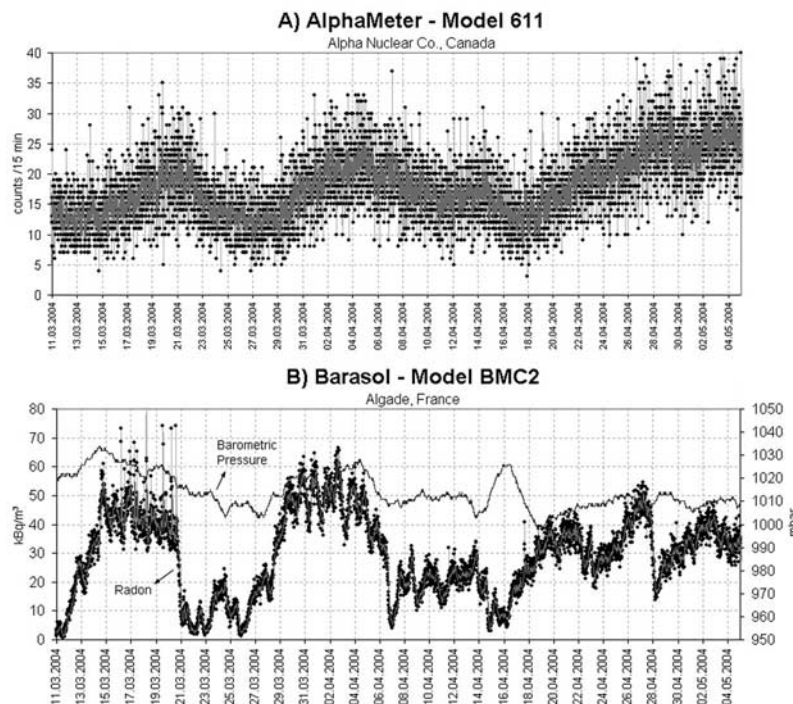


Figure 5. Comparative time variation of soil gas radon data collected by different sensors in the same soil hole at Gaziköy station. A: AlphaMeter, B: Barasol. Blue line in B- is barometric pressure.

electrical conductivity of the spring waters were measured by PCOND meters and appropriate sensors and on-site performance tests were conducted for all components on a monthly basis using calibration standards.

[9] The soil radon data were collected by using AlphaMeter 611 sensors manufactured by AlphaNuclear Co (Canada). The sensors performed quite well for most of the time for the purpose of continuous monitoring. However, some operational issues in the soil environments adversely affected the sensor performance as shown in Figure 4. One unstable power supply (12 V battery) led to unstable sensor performance (Figure 4a). Nearby quarry blasts also led to false readings as shown in Figure 4b, perhaps due to sudden increase in radon release due to the pressure waves because the detector response was stable after blasts. The effects of these two perturbations that could have led to erroneous readings have been eliminated by providing a more stable power supply (12 V battery backed by continuous charge hooked up to the main power line) and by avoiding measurement sites close to quarries. Figure 4c shows one example of a soil radon sensor severely affected by humidity as a result of flooding of measurement site for several days. It seems that condensed water was accumulated on the detector surface leading to possible short-circuits and thus counting of erratic numbers was made (up to 50,000 counts per integration time of 15 m for AlphaMeter and up to several million Becquerel per 15 m integration time for Barasol sensors) that could only be possible in case of short circuiting occurring on the surface of detector (personal communication, with AlphaNuclear and Algade manufacturers personnel 2004). To resolve this issue the sensor was replaced by a new one. However, the replacements caused loss of data for up to one month until the radon buildup in the aerated soil reached equilibrium again.

[10] The data collected by AlphaMeter 611 sensors are given in counts per 15 m integration time. Calibration by the manufacturer provides for the conversion of the count rates into radon activity. For example, as determined by *Thomas et al.* [1992], 10 counts per 15 min of integration time recorded by the AlphaMeter equals to about 20 kBq/m³ soil gas. In this study, we placed a Barasol sensor calibrated in kBq/m³ units alongside an AlphaMeter sensor into the same borehole, about 1 m deep, collecting data simultaneously for a period of three months. The results are shown in Figure 5. The two sensors show a positive correlation in terms of their response to radon in the soil gas: 10 counts recorded by the AlphaMeter correspond to 20 kBq/m³ as recorded by the Barasol. However, the Barasol sensor (detector and/or the electronic component) seems to be affected more by barometric pressure variations thus indicating a less stable and less reliable performance. The inverse correlation between barometric pressure and radon counts that is generally expected often does not hold up, thus complicating the interpretation of the Barasol sensor data (Figure 5). By contrast, the data recorded by the AlphaMeter appear more stable and sudden changes were not recorded. This indicates that the AlphaMeter sensors' performance for long-term continuous monitoring of soil radon data is more satisfactory. Our experience so far suggests that more robust sensors than are currently available would be desirable for continuous seismic observations such as related to seismic activity. Technological improvements that pose a challenge to scientists and engineers are necessary.

[11] The last issue in regard to quality of radon data for use in relation to seismic activity is the possible influence of atmospheric parameters on radon data collected by sensors located in 1 m deep soil environment. Figure 6 shows barometric pressure, rainfall and radon data collected at

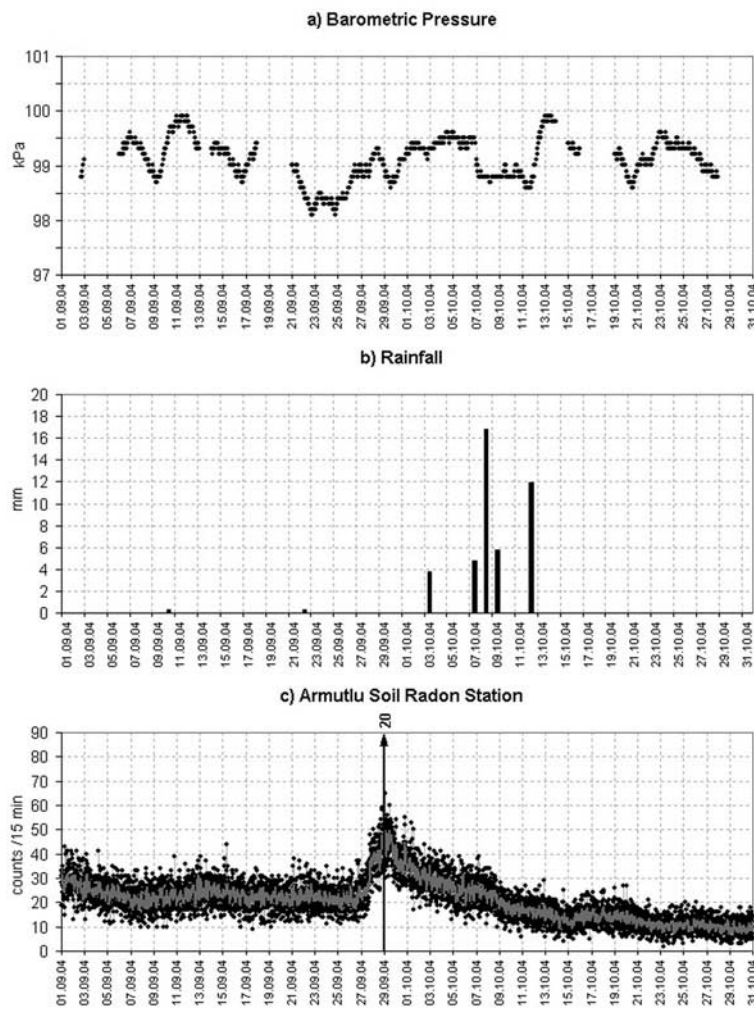


Figure 6. Possible influences of atmospheric parameters on radon data. (a) barometric pressure, (b) rainfall, (c) soil radon data. The anomaly recorded in radon data from 26 to 29 September 2004 suggests a relation to seismic activity. Numbered arrow indicate an earthquake for details see Table 2.

Armutlu radon monitoring station for a period of two months. The results indicate that radon data are not influenced by these two atmospheric parameters and that a recorded radon anomaly lasting from 26 to 29 September 2004 (Figure 6) is clearly related to seismic activity as it will be discussed later. This is a confirmation that pre-cursory signals are intensified and the influence of secondary parameters (e.g., atmospheric) are minimized by locating the radon sensor in a fault zone as suggested by *Chyi et al.* [2001]. In this study, diurnal variations at several radon monitoring stations have also been measured and the results, as demonstrated in Figure 7, suggest that diurnal variation in radon concentration is insignificant.

2.4. Statistical Analysis

[12] In order to model the dynamics of the radon, we have analyzed the soil radon distribution from various sites. Since most of our sites are either seismically active or located on faults continuously emit radon, many radon anomalies were observed. To compare these anomalies with observations from a quiescence site (QS), we set up a reference station, namely Gebze, 4 km away from a known fault. The purpose of this site was to follow the

statistical variations of the radon release at a location without seismic activity of $M > 3$ over a period of six months. Our observations were then compared with the statistical variations seen in data collected during seismically active and inactive periods from other sites closely associated with active faults (e.g., Efteni location). Needless to say, each station has different site characteristics (underlying rock, soil porosity and permeability) leading to site-specific statistical variations of the data. In this study, we consider a single exponential type probability density functions (pdf) and hence examine if the analyzed data fits one of the *Rayleigh*, *Gamma* and *Gaussian* pdf's. The expressions related to these pdf's are given [Papoulis, 1991] as;

$$\begin{aligned} \text{Rayleigh(*)} \quad f(x) &= \frac{x - \gamma}{\alpha^2} \exp\left(-\frac{1}{2} \left(\frac{x - \gamma}{\alpha}\right)^2\right) \\ \text{Gamma} \quad f(x) &= \frac{(x - \gamma)^{\alpha-1}}{\beta^\alpha \Gamma(\alpha)} \exp\left(-\frac{(x - \gamma)}{\beta}\right) \\ \text{Gaussian} \quad f(x) &= \frac{1}{\sqrt{2\pi}\sigma} \exp\left(-\frac{1}{2} \left(\frac{x - \mu}{\sigma}\right)^2\right) \end{aligned}$$

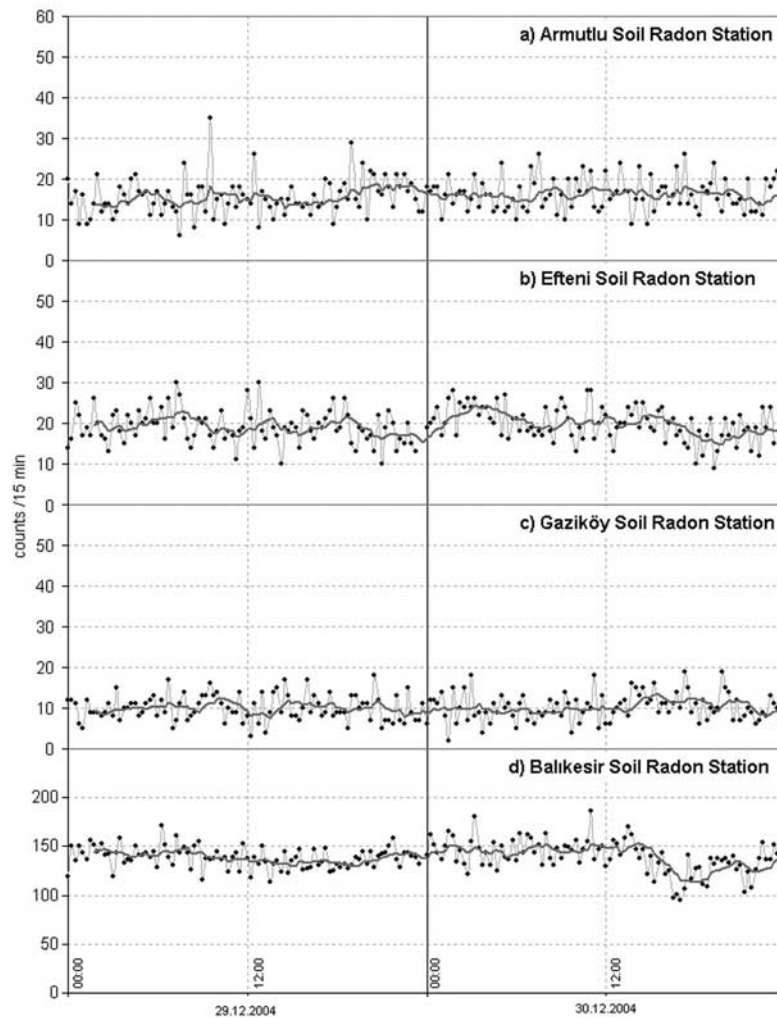


Figure 7. Diurnal variations in soil radon concentration at several radon monitoring stations in the region.

(*)The Rayleigh distribution with parameter α is equivalent to another more general distribution called the Weibull distribution which can be used instead with parameters

$$A = \sqrt{2}\alpha \text{ and } B = 2 : f(x) = \frac{A}{B} \left(\frac{x - \gamma}{B} \right)^{A-1} \exp \left(- \left(\frac{x - \gamma}{B} \right)^A \right)$$

[13] The data collected and analyzed in this study represent the radon intensity level, in other words they represent the number of alpha particles released by the radon gas and counted by a detector over a fixed time interval, in our case 15 m. It is well established that such counting statistics related to particle motion can easily be modeled as a Poisson distribution [Papoulis, 1991]. However, another dominant process prevails here, one based on the upward transport of radon gas through soil. We show that this movement of the gas depends mainly on the physical soil characteristics (such as diffusive paths, fractures, etc.) and that it can be modeled as a random walk process.

[14] Data analysis is performed by selecting the “best” probability density function among several probability den-

sity functions, with a goodness of fit test applied to arrive at the best selection.

3. Results and Discussion

3.1. Time Variation of Soil Gas Radon and Related Seismicity

[15] The seismic activity in the Marmara region during the observation period between 2002–2005 is summarized in Table 2. Total 21 earthquakes were recorded with magnitude greater than M4.0. The locations of the 21 seismic events are given on the map (Figure 1). The largest one, M5.3, occurred outside of the observation area (EQ# 6 in Table 2 and Figure 1).

[16] The spring water monitoring data, namely water temperature, electrical conductivity, water hardness, anion and cation content, suggest that during the observation period (2002–2005) no reliable anomaly was detected in relation to this seismic activity. The chemical compositions of the spring waters were stable and no consistent changes were recorded in the temperature, electrical conductivity, cation, anion, or stable isotopes values of the spring waters

Table 2. Earthquakes With $m_d \geq 4.0$ Occurring Between 2002–2005 in the Marmara Region^a

No	Date (dd.mm.yy)	Local Time (hh:mm:ss)	Latitude (°N)	Longitude (°E)	Magnitude (m_d)	Location
1	28.02.2002	11:37:51	40.8190	28.1233	4.80	Marmara Sea
2	23.03.2002	05:36:10	40.8590	27.8500	4.8	Marmara Sea
3	05.05.2002	11:22:10	40.5550	28.3270	4.3	Marmara Sea
4	08.03.2003	13:18:07	40.6653	30.6142	4.0	Akyazi, Adapazarı
5	09.03.2003	21:01:32	40.7328	30.6205	4.1	Akyazi, Adapazarı
6	20.03.2003	14:25:34	39.9745	28.7655	4.5	Orhaneli, Bursa
7	21.05.2003	11:21:50	40.8690	30.9765	4.5	Gölyaka, Düzce
8	28.05.2003	02:25:32	40.8068	31.0103	4.0	Gümüşova, Düzce
9	09.06.2003	20:44:03	40.2027	27.9685	5.1	Bandırma, Balıkesir
10	09.06.2003	20:47:05	40.2473	27.9408	4.1	Bandırma, Balıkesir
11	06.07.2003	22:10:28	40.4243	26.2055	5.3	Saroz Bay
12	06.07.2003	23:10:13	40.5243	26.0170	4.9	Saroz Bay
13	13.07.2003	08:09:48	40.8570	27.5127	4.0	Marmara Sea
14	23.12.2003	14:23:36	39.8750	29.2317	4.8	Keleş, Bursa
15	27.03.2004	01:59:57	40.8502	31.0465	4.2	Düzce
16	19.04.2004	18:27:16	40.6070	27.7027	4.5	Marmara Island
17	16.05.2004	06:30:48	40.6957	29.3222	4.2	Marmara Sea
18	27.06.2004	18:31:47	40.9280	26.0603	4.5	Turkey-Greece Border
19	13.08.2004	18:13:44	40.8330	26.4372	4.2	İpsala, Edirne
20	29.09.2004	18:42:07	40.7797	29.0200	4.0	Marmara Sea
21	04.11.2005	22:12:08	40.6998	27.2982	4.1	Marmara Sea

^aData from catalogs of TUBITAK MRC and Boğaziçi University Kandilli Observatory and Earthquake Research Institute (KOERI).

prior to any of the earthquakes listed in Table 2. Lack of significant anomalies in the spring waters is interpreted as a sign of insufficient crustal deformation (and thus insufficient water-rock interaction) during the observation period consistent with the fact that only relatively small to medium sized earthquakes occurred in the region.

[17] During the same observation period, however, variations in soil radon concentration were observed; suggesting that rate of radon emanation in soil is more easily influenced, compared to underground water, prior to medium-size earthquakes. Continuous radon measurements at 15 min interval was conducted to ensure possible short duration anomalies before earthquakes were not missed in this study as reported elsewhere in case of non-continuous measurements [Toutain and Boubroun, 1999; Chyi *et al.*, 2001]. Radon was found to be more responsive to seismic activity and to earthquakes $M > 4$, which were preceded by a positive anomaly, e.g., an increase in radon concentration in most radon stations located up to 100 km in distance from the nearest earthquakes. Some selected time series of soil radon data are presented in Figure 8. The dates of the earthquakes with $M > 4$ shown on map in Figure 1 and listed in Table 2 are superimposed on the figures in order to show the correlation between soil radon concentration changes and seismic activity. The time variations of soil radon that could be related to seismic activity typically includes three stages: 1) build-up, 2) high level, and 3) decrease to background level, depending on the epicentral distance of the impending earthquake to the station.

[18] Figure 8a shows the time variation of soil radon at the Gaziköy station at the western end of the Marmara Sea where the fault rejoins the land. Here, the positive radon anomaly prior to EQ # 11 lasted for about 13 days with the epicentral distance of this earthquake to the station being 100 km. This station is in a seismically active zone and numerous small seismic events occur almost continuously, resulting in quite variable background variations due to the response of the radon to this continuous seismic activity.

Here it is quite possible that earthquakes coming in train may have reinforcing and destructing interferences and may make precursory signals difficult to identify as suggested by Chyi *et al.* [2001].

[19] In Figure 8b, positive soil radon anomalies recorded at Armutlu station are shown prior to Eq # 1, 2 and 3 (Table 2). Other positive anomalies are related to smaller, close-by earthquakes (unnumbered but within 60 km of the station). The same positive soil radon responses prior to same earthquakes was detected in Gölcük (Şarköy) station as depicted in Figure 8c. The background data at this location show relatively large radon variations, probably due to the continuous small seismic activity in the western end of the Marmara Sea close to this station.

[20] It is quite apparent from the above discussion that there seems to be a trade-off between the location of the radon station and the distance to the epicenter of the earthquake and also the duration of the radon anomaly for a given earthquake magnitude. The temporal variations of the radon data from the Efteni (Düzce) station shown in Figure 8d reinforces this apparent trade-off relation between distance to the epicenter and duration of the radon anomaly. The epicentral distance of EQs # 4 and 5 (M_4 and $M_{4.1}$, respectively) to the radon station are about 50 km and the radon anomalies detected before these events show an abrupt increase. By contrast, EQs # 7 and 8 ($M_{4.5}$ and M_4 , respectively) occurred within 15 km of the radon station. It is noteworthy that the anomaly peak was wider and there is a time lag between the radon peak and the time of the seismic event: the earthquake occurred about 25 days after the highest radon signal. On the other hand, the radon anomaly prior to EQ # 14 ($M_{4.8}$) with an epicentral distance of about 140 km resulted in narrow peak lasting for only 7 days. The epicentral distances of EQs # 9, 10, 11, 12 and 13 to the Efteni station were more than 200 km. We chose to plot these EQs with dashed lines suggesting that a clear relation between those events and the radon data at the Efteni station could not be established, due to the large

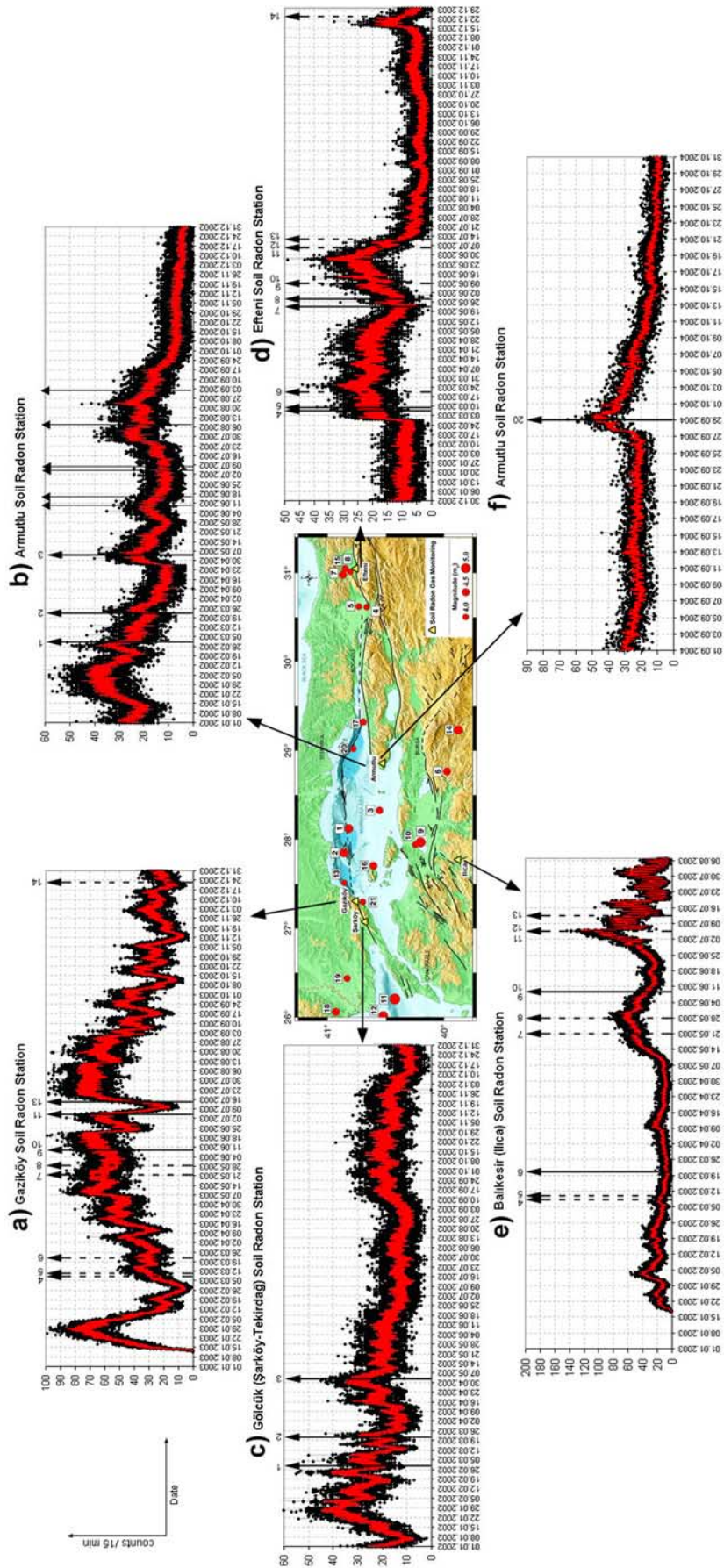


Figure 8. Time variation of soil radon (in counts/15 m) from (a) Gaziköy-Şarköy (Tekirdağ), (b) Armutlu (Yalova), (c) Gölcük-Şarköy (Tekirdağ), (d) Efteni-Gölyaka (Düzce), (e) Ilıca (Balıkesir), (f) Armutlu (Yalova) continuous monitoring stations. Numbered earthquakes shown in solid lines are the ones with $4.0 \leq M < 5.3$ occurring at a distance less than 150 km from the observation site. Earthquakes shown with dashed lines are ones with $M \geq 5.3$ occurring at a distance more than 150 km from the observation site. Unnumbered solid lines are for the earthquakes with magnitude < 4.0 but at a distance less than 60 km to the observation site. For numbered earthquakes details are given in Table 2.

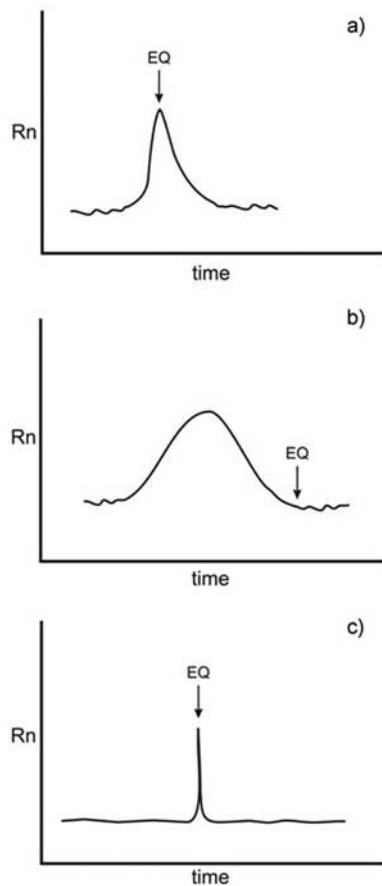


Figure 9. An example of time variation of radon data from a continuous soil gas radon monitoring site prior to (a) nearby earthquakes (≤ 150 km) with $4.0 \leq M \leq 5.3$, (b) close earthquakes (<60 km) with $4.0 \leq M \leq 5.3$, (c) distant earthquakes (> 150 km) with magnitude between 4.0 and 5.3.

distances. The radon anomalies between mid-May to end of June is probably related to small events, maybe aftershocks to the EQ #7 of M5.3, but not related to the distant earthquakes EQs # 9, 10, 11, 12 and 13.

[21] The Balıkesir Ilica soil radon station is located in a geothermal area and its time variations in soil radon are presented in Figure 8e. EQs # 4, 5, 7, and 8 are between M4.0 and M4.5 and occurred more than 150 km to the east of the station. They are shown as dashed lines. EQs # 9 and 10 occurred about 30 km from the station and their radon data show rather strong anomalies prior to these events. EQs # 11 and 12 occurred about 145 km northwest of the radon station in the Saroz Bay, but due to the relatively large magnitude of the earthquake, M5.3, a positive anomaly is clearly discernable. The different time evolution patterns of the radon anomaly peaks before EQs # 9, 10 and 11 is worth noting. Since the epicentral distance of EQ# 9 (M4.8) to the station was only about 30 km, the monitoring site was obviously affected for a relatively long period of time by the deformation process, thus producing a positive radon anomaly that lasted longer, about 30 days, than that prior to the EQs #10 and 11, which followed the maximum of the radon signal by a longer time interval. This may be interpreted as

to indicate that, whatever the mechanism responsible for the radon release, it created a longer time lag between the maximum radon signal and the earthquake. Taking a purely mechanistic approach, this may be explained by the closure of microcracks during deformation and thus reduction of the radon emanation. However, the epicentral distance of EQ #11 to the Balıkesir Ilica station was about 145 km, but the recorded radon anomaly was sharp and the earthquake occurred when the radon signal was at its maximum. This seems to suggest that the deformation field related to the impending earthquake # 11 in the Saroz Bay took time to reach the station and that the soil radon concentration anomaly lasted for about 9 days.

[22] The temporal variation of the soil radon data from Armutlu station showing a clear response to EQ # 20 (M4.0) is given in Figure 8f. Prior to this earthquake which has an epicentral distance to the monitoring station of about 50 km, we observe a narrow, sharp anomaly lasting for about two days.

[23] The observations presented above strongly suggest that, at least for this section of the North Anatolian Fault and for the magnitudes of earthquakes recorded during the observation period, variations in the soil radon data are a useful earthquake precursor. As already observed by *Sultankhodhaev* [1984], for a given observation site, the duration of the positive radon anomaly depends primarily 1) on the magnitude of the impending earthquake and 2) on the distance to the epicenter. The amplitude and width of radon anomaly peak depends primarily on the earthquake magnitude and epicentral distance from the observation site. The precursory radon anomaly lasts longer the larger or the closer the earthquake. It is shorter the smaller or farther away the impending event. On the basis of these observations, Figure 9 depicts the general peak shape of the radon anomaly prior to large and small, far and close-by earthquakes. For given magnitude earthquake ($4.0 \leq M \leq 5.3$), as the epicentral distance to the monitoring site increases, the anomaly peak gets narrower (e.g., duration of anomaly is shorter). As the epicentral distance to the monitoring station decreases, the anomaly peak gets broader (e.g., duration of anomaly preceding earthquake is longer).

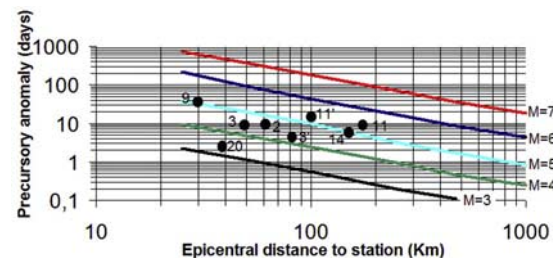


Figure 10. Possible relation between precursory soil radon anomaly D (days), epicentral distance of earthquake (km) and magnitude (M) of earthquake based on equation (1) ($\log(DM) = 0.63M + (-0.15)$; [*Sultankhodhaev*, 1984]). Data for 6 earthquakes discussed in this study and listed in Table 2 are plotted. 3 and 3 “are data for EQ# 3 from Armutlu and Gölcük (Şarköy) radon stations, respectively. 11 and 11” are data for EQ# 11 from Balıkesir Ilica and Gaziköy (Şarköy) stations, respectively.

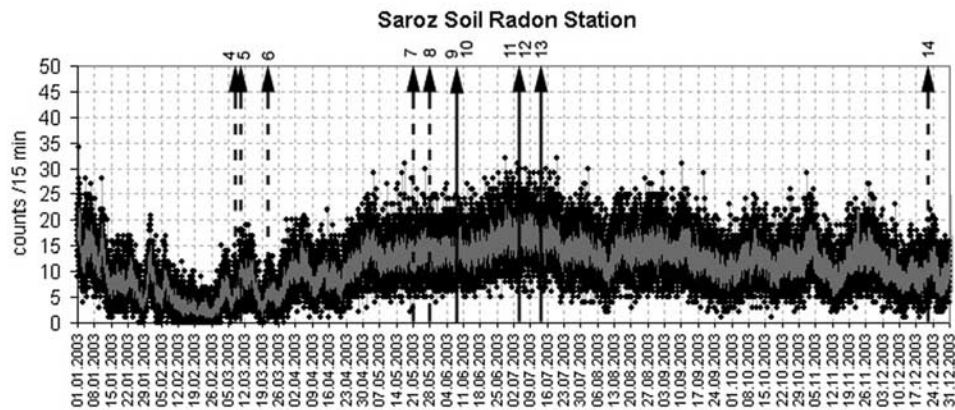


Figure 11. Time variation of soil gas radon at Saroz continuous monitoring station.

[24] An empirical relationship between the precursory time T (in days) and the epicentral distance D (in km) to the magnitude (M) is given by the following expression:

$$\log(DT) = 0.63M + b \quad (1)$$

where b has been proposed to be -0.15 [Sulthankhodaev, 1984; Planinic et al., 2004]. Figure 10 shows a plot depicting the relation given in equation (1). The Magnitude (M), epicentral distance (D) and precursory radon anomaly times (T) for some of the earthquakes and radon data discussed in this paper are superimposed. The data represented cover the precursory radon anomaly for observed earthquakes with magnitudes between 4 and 5.3 and with an epicentral distance to the measuring station up to 150 km. The results suggest that the relationship given by equation (1) roughly holds for the Marmara region and for earthquakes $M < 5.3$. However, as more data are collected from increasing number of radon stations and as more earthquakes occur in the region, we believe it will be possible to refine equation (1) and it may become region specific. The question whether this relationship will also hold for larger events can only be answered after such earthquakes have occurred in the region under study.

[25] The above relationship between the time variations of soil gas radon and seismic activity has been discussed for data collected by monitoring stations located in areas of compressional regimes as also shown by Birchard and Libby [1978]. However, this empirical relationship de-

scribed here appears not to hold for other subtectonic regimes such as transtensional and/or extensional domains where radon seems not to be responsive to seismic activity. Figure 11 shows a time variation of soil gas radon from a station located in an area with transtensional regime. No relation is found between the radon anomaly and seismic activity. In Table 3, a summary of the responsiveness of radon to seismic activity based on the geological characteristics of the monitoring sites is listed. It can be argued that, while the basement rock lithology appears not to play a role, the tectonic regime is the dominating factor. Compressional regimes provide for the tightest radon-seismicity correlation. Monitoring stations located in transtensional and/or extensional regimes with geothermal activity also lead to good response of the radon data to seismicity. Extensional regimes with no geothermal activity are probably not good sites for soil radon monitoring because the response of radon to seismicity has been found to be weak to non-existing as demonstrated in Figure 11.

[26] As shown above, a good relation between ground radon gas anomaly and seismic activity has been observed, however, it must be clearly stated that radon data (or any technique) alone should never be considered sufficient to indicate coming of an earthquake which is by definition a complex natural phenomenon. Therefore multiparameter observations (geochemistry of gas and water emanating from active faults, crustal deformation data, microseismology, electric, electromagnetic and many others) should be conducted with patience and for long time until sufficient

Table 3. Geological Features of the Soil Radon Monitoring Stations and Responsiveness of the Soil Radon to Seismic Activity

Soil radon station	Bedrock	Fault/Fracture	Tectonic regime	Geothermal activity	Responsiveness of radon to seismic activity
Saroz	Sedimentary	Yes	Extensional/Transtensional	No	None
Balıkesir Ilıca	Metamorphics	Yes	Extensional	Yes	High
Armutlu	Metamorphics	Yes	Extensional	Yes	High
Gölcük/İzmit	Sedimentary	Yes	Transtensional	No	None to Low
Efteni	Volcanics	Yes	Extensional	Yes	High
Gönen	Volcanics	Yes	Transpressional/compressional	No	High
Kestel/Bursa	Sedimentary	Yes	Transpressional/compressional	No	High
Gölcük/Şarköy	Sedimentary	Yes	Transpressional/compressional	No	High
Gebze ^a	Sedimentary	No	Transpressional	No	None

^aThis site is 4 km away from the strike main strike slip fault segment and has been established for purpose of collecting soil radon data from a passive site.

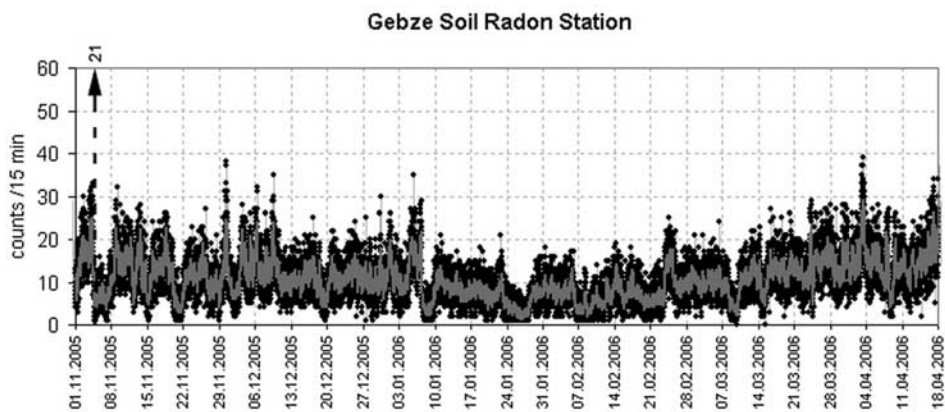


Figure 12. Time variation of soil gas radon at Gebze continuous monitoring station.

data are acquired to develop a working model to convince the scientific community and reach a consensus.

3.2. Statistical Analyses of Radon Data

3.2.1. Analyses of Radon Data for A Quiescent Site (QS)

[27] The soil radon gas data recorded in the reference station Gebze for approximately six months with a 15 m sampling interval yielding 16,000 samples are shown in Figure 12. Using these data and their histograms, we estimate the parameters for *Rayleigh*, *Gamma* and *Gaussian* pdfs using the popular maximum likelihood method. The normalized histogram of the data and the fit-pdfs (solid red lines) are plotted in Figure 13 and the estimated parameters with the goodness of fit test results are provided in Table 4

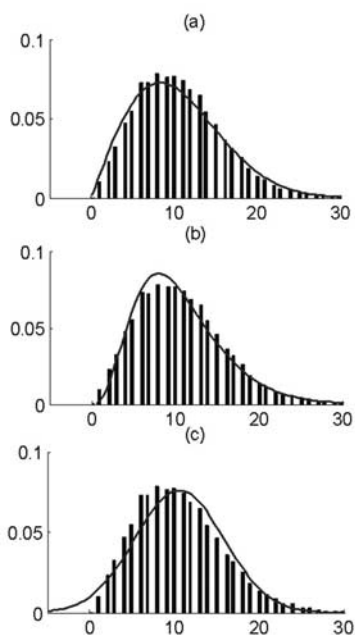


Figure 13. The histogram of the Gebze radon data (01 November 2005–17 April 2006) and the pdf fits (red solid lines) in order: (a) Rayleigh, (b) Gamma, (c) Gaussian. The best fit is Rayleigh (See Table 4).

where the best fit is found to be the Rayleigh density function.

[28] In order to investigate the behavior of the shorter segments of the same data (i.e., 2800 samples \sim 1 month) the same procedure is applied to the segment corresponding to the dates between 2 November 2005 and 1 December 2005. It turns out that the probability density function of the overall data is still stationary for such shorter segments, i.e., the best fit, as expected, appear to be in the same rank order as the data corresponding to longer term.

[29] Since Gebze is selected as the reference station, the corresponding Rayleigh-type distribution can be assumed to be the reference distribution. In other words, any deviation from Rayleigh-type distribution can be attributed as an anomaly.

3.2.2. Analyses of Radon Data for Seismically Quiet Period (SQP) at Active Fault Site

[30] When the analysis is extended to other stations, similar behavior for non-seismic periods is observed. For example, the overall data collected in Efteni site between 02 November 2003 and 15 December 2003 shown in Figure 14 is known to be quiet during which no seismic activity above $M>3$ is recorded. The corresponding histogram and its pdfs for this period are shown in Figure 15, and the estimated parameters are given in Table 5 where, similar to the previous observations, the best fit is found to be the Rayleigh density function as well.

3.2.3. Analyses of Radon Data for Seismically Active Period (SAP) at Active Fault Site

[31] In order to investigate the pdf characteristics of the soil radon gas data during the Seismically Active Period

Table 4. Probability Density Functions and the Estimated Parameters for Gebze Data (01 November 2005 – 17 April 2006)

Rank #	Name	Estimated Parameters	Goodness of Fit (least-squares) ^a
1	Rayleigh	$\sigma = 8.3581 \quad \gamma = 0$	0.00876
2	Gamma	$\beta = 4.0963 \quad \alpha = 2.587 \quad \gamma = 0$	0.00988
3	Gaussian	$\mu = 10.5973 \quad \sigma = 5.2358$	0.04300

^aLeast square error between empirical and fit cumulative density functions (CDF). The parameters used by CDF are estimated using a standard maximum likelihood method and a least-squares error is defined as the difference between the empirical and parameter based CDF. The best fit, then, is obtained by ranking the minimum error in the least-squares sense.

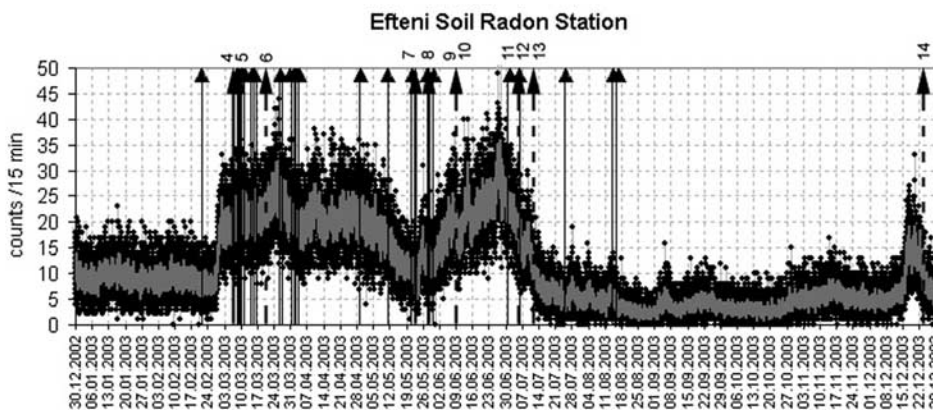


Figure 14. Time variation of soil gas radon at Efteni continuous monitoring station.

(SAP), the active period of Efteni data between 12 February 2003 and 08 March 2003 were analyzed. The data include radon emanation recordings just before earthquakes # 4 and 5 (Table 2) with $M = 4.0$ and $M = 4.2$ in Akyazı which is about 40 km west of the Efteni site. The histogram in Figure 16 appears to have two peaks suggesting at least two processes with possibly exponential family distributions. This verifies that the seismic activities affect the level of Radon gas emanation leading to multiple densities.

[32] Another example is for the transient behavior of the Efteni site (between 30 November 2003–21 December 2003, approximately 2800 points). The histograms and the best fit pdf’s as given in Figure 17 show that there is distinct separation from Rayleigh-type distribution. It is useful to

note that even a visual evaluation of the histogram of this data may suggest a mixture distribution.

[33] A final example in terms of the distributions for the co-seismic period (where several earthquakes followed each other) is given in Figure 18 where the histograms of the Efteni radon data (03 March 2003–17 July 2003) and the pdf fits are presented. In this case while the best fit is Gaussian and the worst fit is Rayleigh. The goodness of fit results can be compared in Table 6. This seems to suggest multiple events (repeated seismic activities) forcing the distribution toward Gaussian (due to the “law of large numbers”).

3.2.4. Possible Physical Meaning of the Observations

[34] The analysis of the reference site suggests that Rayleigh is the most likely pdf for “normal” behavior of soil radon gas release. Rayleigh pdf can be explained in terms of random walk processes [Papoulis, 1991]. In general a random walk process is described as motion of matter whose direction is random in successive time intervals.

[35] It seems that, during a seismic period, the radon gas moves through soil and approaches to the sensor by showing a random walk behavior which corresponds to a Rayleigh-type exponential distribution function. When the gas arrives nearby the sensor, the alpha particles hit the sensor surface obeying a Poisson distribution. The total compound process appears as having Rayleigh-type distribution. However, during earthquake preparation phase, probably by 1) changes in permeability of the soil and underlying rocks due to micro-fracturing of rock under increasing elastic stress and/or 2) increase in gas concentration leads to positive anomalies in radon time series (Poisson distribution of the increasing alpha particles tend to normal distribution) and the behavior of the data is quite

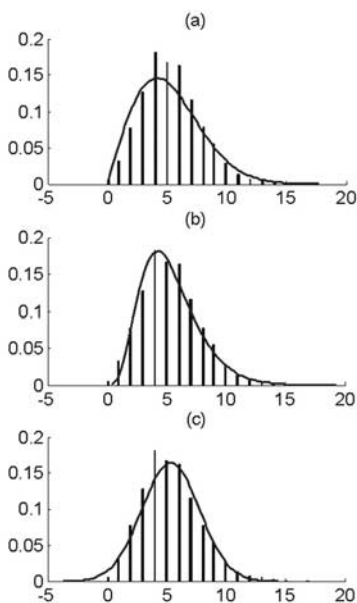


Figure 15. The histogram of the Efteni radon data (02 November 2003-15 December 2003) and the pdf fits (red solid lines): (a) Rayleigh, (b) Gamma, (c) Gaussian. In this case Gamma is the worst fit whereas the best fits are in order Rayleigh and Gaussian. (See Table 5)

Table 5. Pdf and the Estimated Parameters for a Segment of Silent Segment for Efteni Site^a

Rank #	pdf	Estimated Parameters	Goodness of Fit (least-squares)
1	Rayleigh	$\sigma = 4.1466 \quad \gamma = 0$	0.0156
2	Gaussian	$\mu = 5.3396 \quad \sigma = 2.4242$	0.0463
3	Gamma	$\beta = 4.8505 \quad \alpha = 1.1008 \quad \gamma = 0$	0.0797

^a(02 November 2003 – 15 December 2003).

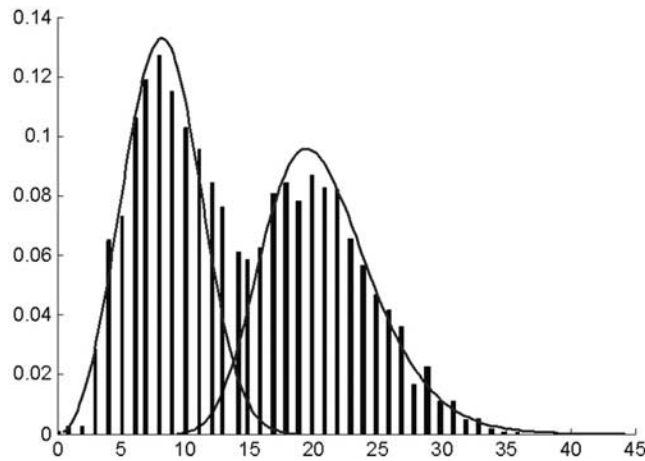


Figure 16. The histogram of the Efteni radon data (12 February 2003–05 March 2003). Note that there are more than one process yielding two (possibly exponential family) pdfs.

far from Rayleigh-type distribution, toward either Gaussian-type or mostly toward a mixture model of distributions. Further analysis using recently developed signal processing techniques [Baykut *et al.*, 2007] may yield better understanding and modeling of the -behavior of the- radon data.

4. Conclusions

[36] A good relation between ground radon gas anomaly and seismic activity has been observed for the last three years in the Marmara region. Although with varying degree of influence on the radon activity, the controlling factors, as widely known, are numerous. However, the data collected from all radon gas monitoring stations since 2001 suggest that 1) basement geology, 2) existence of deep water circulation (e.g., geothermal activity), and 3) structural features (compressional or extensional/dilatational regime)

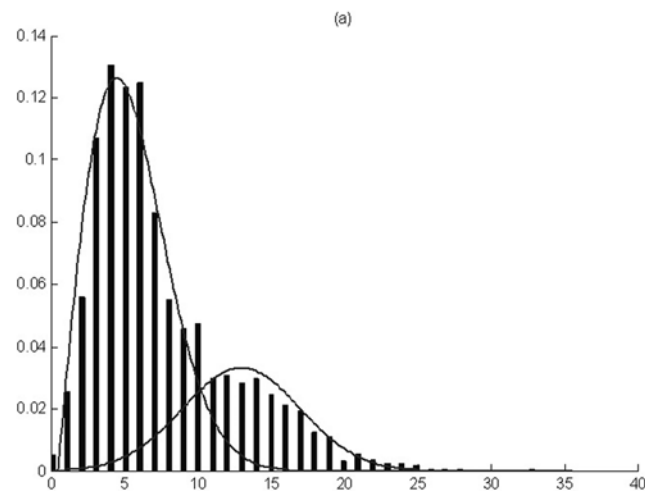


Figure 17. Visual evaluation of the histogram of the Efteni radon data (between 30 November 2003–21 December 2003) suggests a mixture distribution.

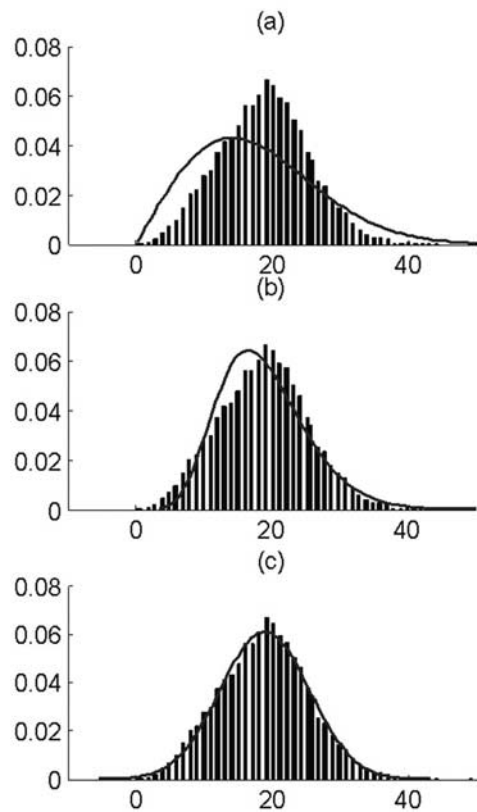


Figure 18. The histogram of the Efteni radon data (03 March 2003–17 July 2003) (Co-Seismic Period) the pdf fits (solid line): (a) Rayleigh, (b) Gamma, (c) Gaussian. Note that in this case the best fit is Gaussian. The worst fit is Rayleigh. (See Table 6)

of the observation sites have prime influence on the radon gas variations in the earthquake preparation period. Atmospheric conditions play only a secondary role. Thus site selection for continuous radon gas monitoring is very important, and when appropriately determined, results in successful observations. Monitoring stations established on the active fault segments associated with 1) zone of compression involving sedimentary rocks and/or 2) zones of dilatation with deep water circulation in any type of basement rocks have systematically yielded the closest relation (positive correlation) between radon gas anomaly and earthquake activity (magnitude between 4.0 and 5.3) for epicentral distance of up to 150 km during the observation period in the region.

[37] The radon data collected during seismic quiescence periods statistically show Rayleigh-type exponential probability density functions (pdf) which may be regarded as the

Table 6. Pdf and the Estimated Parameters for a Segment of the Efteni Radon Data (03 March 2003–17 July 2003) (for the Co-Seismic Event)

Rank #	pdf	Estimated Parameters	Goodness of Fit (least-squares)
1	Gaussian	$\mu = 18.8823 \sigma = 6.5483$	0.01310
2	Gamma	$\beta = 8.3142 \alpha = 2.2711 \gamma = 0$	0.02070
3	Rayleigh	$\sigma = 14.1319 \gamma = 0$	0.20700

result of random-walks of gas in the permeable and porous soil medium and the Poisson process behavior of the alpha particles. However, the radon data collected prior to earthquakes where the radon time series show positive anomaly (possible precursor to earthquake), the radon data display different characteristics with a deviation from Rayleigh-type pdf toward a mixture of distributions mostly. This lends support to inference that the pathways of the gas movement prior to earthquake are influenced possibly by increased microfractures related elastic deformation and this process results in increased radon concentration manifested as positive radon anomaly.

[38] The good relation shown between ground radon gas anomaly and seismic activity should be considered only an encouraging state and never considered sufficient to indicate coming of an earthquake which is by definition a complex natural phenomenon. Therefore multiparameter observations (geochemistry of gas and water emanating from active faults, crustal deformation data, microseismology, electric, electromagnetic and many others) should be conducted with patience and for long time until sufficient data are acquired to develop a working model to convince the scientific community and reach a consensus.

[39] **Acknowledgments.** The authors thank Istanbul Metropolitan Municipality and TUBITAK Marmara Research Center for the financial support. Special thanks are extended to Kevin Cuff (University of California, Berkeley) for technical help during early stages of this study. We also thank our colleagues at TUBITAK Marmara Research Center, Earth and Marine Sciences Institute, namely, Süleyman Canan, Onur Tan, Alpaz Belgen, Raşan Çakmak, Salih Akar, Levent Kurt, Hakan Yakan, Muhiddin Çergel, Reşad Kafarov for technical assistance provided in this study. Cengiz Gezer from Istanbul Technical University provided support in processing of the data. Finally, colleagues from Istanbul Metropolitan Municipality, Kemal Duran, Hikmet Karaoğlu and Mr. Salim Gümüş, are thanked for continuing interest and support in this study. Richard Arculus and Antonio Rapolla are thanked for the editorial handling. Friedemann Freund and an anonymous reviewer provided careful reviews and valuable suggestions that greatly improved the manuscript.

References

- Barka, A., and K. Kadinsky-Cade (1988), Strike slip fault geometry in Turkey and its influence on earthquake activity, *Tectonics*, *7*, 663–684.
- Baykut, S., T. Akgül, and S. Ergintav (2007), Estimation of Spectral Exponent Parameter of 1/f Process in Additive White Background Noise, *EURASIP Journal of Advances in Signal Processing*, Vol. 2007, Article ID 63219, 7 pg, doi:10.1155/2007/63219.
- Birchard, G. F., and W. F. and Libby (1978), Earthquake radon anomalies—possible mechanisms, *EOS Trans. AGU*, *57*, 957.
- Chyi, L. L., C. Y. Chou, T. F. Yang, and C.-H. Chen (2001), Continuous radon measurements in faults and earthquake precursor pattern recognition, *Western Pacific Earth Sci.*, *1*(2), 43–72.
- Claesson, L., A. Skelton, C. Graham, C. Dietl, M. Moerth, P. Torssander, and I. Kockum (2004), Hydrogeochemical changes before and after a major earthquake, *Geology*, *32*, 641–644.
- Flerov, G. N., A. M. Chirkov, S. P. Tretyakova, L. V. Dzholos, and K. I. Merkina (1986), The use of radon as an indicator of volcanic process, *Earth Phys.*, *22*, 213–216.
- Freund, F. (2002), Charge generation and propagation in igneous rocks, *J. Geodyn.*, *33*, 543–570.
- Geller, R. J., D. D. Jackson, Y. Y. Kagan, and F. Mulargia (1997), Earthquakes cannot be predicted, *Science*, *275*, 1616–1617.
- Hartmann, J., and J. K. Levy (2005), Hydrogeological and gasgeochemical earthquake precursors—A review for application, *Nat. Hazards*, *34*, 279–304.
- Hauksson, E. (1981), Radon content of groundwater as an earthquake precursor: Evaluation of worldwide data and physical basis, *J. Geophys. Res.*, *86*, 9397–9410.
- Hauksson, E., and J. G. Goddard (1981), Radon earthquake precursor studies in Iceland, *J. Geophys. Res.*, *86*, 7037–7054.
- Heiligmann, M., J. Stix, G. Williams, B. Sherwood, and G. Garzon (1997), Distal degassing of radon and carbon dioxide on Galeras volcano, Colombia, *J. Volcanol. Geother. Res.*, *77*, 267–283.
- King, C. Y. (1986), Gas geochemistry applied to earthquake prediction: A review, *J. Geophys. Res.*, *91*, 12,269–12,281.
- King, J. Y., Y. Koizumi, and Y. Kitagawa (1995), Hydrogeochemical anomalies and the 1995 Kobe earthquake, *Science*, *269*, 38–39.
- Martin-Luis, C., M. L. Quesada, A. Eff-Darwich, J. DelaNuez, and J. Coello (2002), A new strategy to measure radon in an active volcanic island (Tenerife, Canary Islands), *Environ. Geol.*, *43*, 72–78.
- Papoulis, A. (1991), *Probability, Random Variables, and Stochastic Processes*, 666 pp. Mc-Graw-Hill.
- Planinic, J., V. Radolic, and B. Vukovic (2004), Radon as an earthquake precursor, *Nucl. Instrum. Methods Phys. Res. A*, *530*, 568–574.
- Rangin, C., E. Demirbağ, C. İmren, A. Crusson, A. Normand, E. Le Drezen, and A. Le Bot (2001), *Marine Atlas of the Sea of Marmara (Turkey)*, IFREMER, ISBN 2-84433-068-1.
- Sultankhodhaev, G. A. (1984), Earthquake Prediction, *UNESCO, Paris*, 181–191.
- Şaroğlu, F., Ö. Emre, and İ. Kuşçu (1992), *Active Fault map of Turkey (1:2 000 000 scale)*, General Directorate of Mineral Research and Exploration (MTA), Ankara, Turkey.
- Thomas, D. M., J. M. Cotter, and D. Holford (1992), Experimental design for soil gas radon monitoring, *J. Radioanal. Nucl. Chem.*, *161*, 313–323.
- Toutain, J. P., and J. C. Baubron (1999), Gas geochemistry and seismotectonics: A review, *Tectonophysics*, *304*, 1–27.
- Turcotte, W. L. (1991), Earthquake prediction, *Annu. Rev. Earth Planet. Sci.*, *19*, 263–281.
- Virk, H. S., and B. Singh (1993), Radon anomalies in soil gas and groundwater as earthquake precursor phenomena, *Tectonophysics*, *227*, 215–224.
- Wakita, H. (1996), Geochemical challenge to earthquake prediction, *Proceed. Natl. Acad. Sci. USA*, *93*, 3781–3786.
- Wakita, H., Y. Nakamura, and Y. Sano (1988), Short-term and intermediate-term geochemical precursors, *Pure Appl. Geophys.*, *125*, 267–278.

T. Akgül, S. Ergintav, S. İnan, R. Saatçılar, and C. Seyis, TUBITAK Marmara Research Center, Earth and Marine Sciences Institute, Gebze-Kocaeli, Turkey. (tayfun.akgul@itu.edu.tr; semih.ergintav@mam.gov.tr; sedat.inan@mam.gov.tr; ruhi.saatcilar@mam.gov.tr; cemil.seyis@mam.gov.tr)

M. Baş, Istanbul Metropolitan Municipality, Department of Earthquake and Ground Investigations, Saraçhane, İstanbul, Turkey. (mbas@ibb.gov.tr)

S. Baykut, Istanbul Technical University, Department of Electronics and Communications Engineering, Maslak, İstanbul, 34469, Turkey. (suleyman.baykut@itu.edu.tr)